Technische Universiteit
Eindhoven
University of Technology

Department of Mechanical Engineering

Advanced motion control (4CM60)

Exercise set 3

Student name:	**Student ID:**
Tom van de Laar	1265938
Job Meijer	1268155

Version 1

Eindhoven, June 2019

Exercise 3.15

This exercise is about frequency domain ILC applied to a printer system. Before the actual exercise is discussed the given system is analyzed. The loaded data contains a discrete and a continuous controller for the discrete model of the printer. A sampling frequency of 1 kHz is used for the measurements. The nyquist frequency is defined as half the sampling frequency. Therefore, the nyquist frequency is 500 Hz. The sensor is placed at a non-collocated position. The model is on the boundary of stability duo to eigenvalues of A which are located on the unit circle. The controller can be seen as a lead-lag filter combined with a low pass. Where, first the a lead is applied followed by the lag. The order of the controller is two. The nyquist plot of the closed-loop system indicates a stable closed loop. With a bandwidth of 9 Hz a gain margin of 6.2 dB, phase margin of 48 deg and Modulus margin of about 6 dB.

a) When performaing a simulation with the feedback controller setting N trails equal to 1. The achieved maximum error is $3.26 \cdot 10^{-3}$ meters and the two norm of the error is equal to $7.67 \cdot 10^{-2}$.
b) Next, a mass feedforward term is applied to the system. First a value for the mass m is derived, based on G as can be seen in figure 1. Now the feedforward is applied as $f = C^{ff}\ddot{r}$. The achieved maximum error is now $5.14 \cdot 10^{-4}$ meters and the two norm of the error is equal to $1.29 \cdot 10^{-2}$.

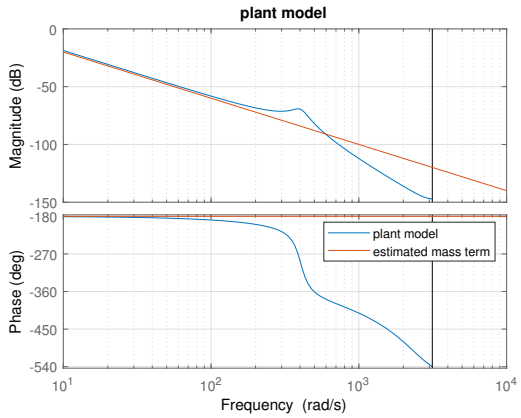

(a)

Figure 1: Mass estimation

c)For the next exercise a frequency domain ILC controller is designed. Herefore, an causal Lc and non causal L is constructed. Lc should be an approximation of $(GS)^{-1}$, the better the approximation of $(GS)^{-1}$ the further the error can be reduced by appling the ILC term. The zero phase error tracking control(ZPETC) approach is used to approximate the inverse of the process sensitivity. GS can be written in terms of stable and unstable zero's as in equation 1. Where, z^{-d} is the delay, B_s are the stable zeros and B_u are the unstable zeros.

$$GS(z^{-1}) = \frac{z^{-d}B_s(z^{-1})B_u(z^{-1})}{A(z^{-1})} \tag{1}$$

Based on the previous equation a non-causal L is constructed as in equation 2. Where, $B_u(z) = z^p B_u^*(z^{-1})$. From this equation the anti-causal part can be extracted from the equation, as in equation 3

$$L(z^{-1}) = \frac{z^d A(z^{-1}) z^p B_u^*(z^{-1})}{\beta B_s(z^{-1})} \tag{2}$$

$$L(z^{-1}) = z^{p+d} L_C \tag{3}$$

In figure 2a the inverse approximation of the process sensitivity, L is plotted. In figure 2b the quality of the inverse approximation can be checked. The magnitude of both the causal and non-causal L drop to ≈ -7 dB for the nyquist frequency, which is 500 Hz. However, below 60 Hz the inverse is almost zero dB, which means LGS ≈ 1. This indicates that the inverse is a good approximation for low frequencies. Furthermore, the phase of the non-causal system is equal to zero. However, when the the delay is added to make L causal the phase drops, as can be seen in the figure 2b. The z^{p+d} is determine by the number of unstable zeros, which introduces the z^p. In this case z^p is equal to one. The z^d is the delay in the process sensitivity, which can be determined by the difference between the number of poles and zeros. In this case the process sensitivity has 5 zeros and 7 poles introducing a delay z^d of two. Therefore, the anti-causal term in L z^{p+d}, is equal to 3. The order of a model is the minimal number of states that a system has in state-space. Therefore, the order of our L_c is equal to 8.

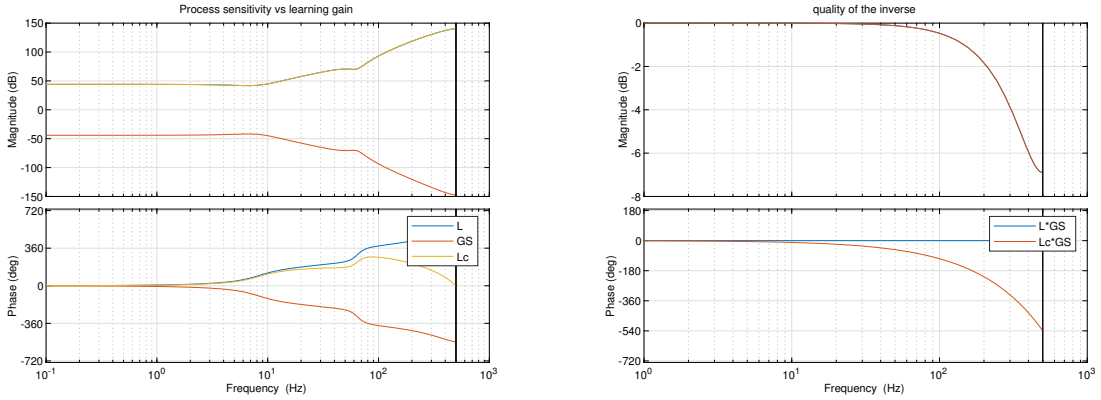

(a) GS and approximated inverse of GS

(b) quality of L and L_c

Figure 2: Inverse approximation of the process sensitivity

d) The convergence of an ILC scheme can be checked by the condition, $|(1 - LG)|<1$. The model for the ILC scheme is the process sensitivity of the original scheme (GS). In figure 3a can be seen that the system is convergent for the model that is used. However, the FRF measurements of the system might lead to a non converging ILC scheme. As can be seen in 3a especially the frequencies above 100 Hz are causing problems.

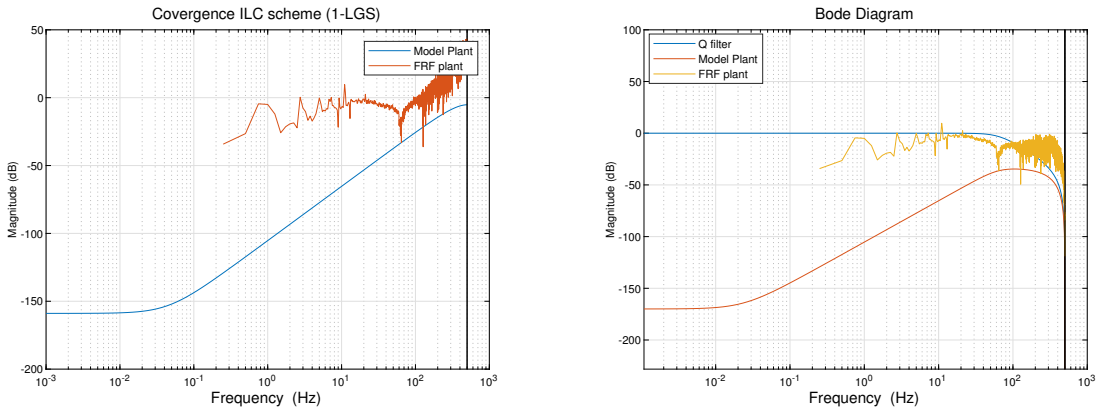

(a) Convergence check ILC scheme

(b) Convergence with robustness filter

Figure 3: Convergence of the ILC scheme

e) A robustness filter is introduced to ensure convergence for both the model and the Frequency Response Function. A butterworth filter is used to filter the higher frequencies. In figure 3b can be seen that now the convergence condition, $|(1 - LG)|<1$, is met for all frequencies, expect for a few spikes at low frequencies. However, due to poor signal to noise ratio these frequencies can be ignored. //
f) Now the ILC controller is implemented on the printer simulation. The causal controller L_c is applied to the error. The new The 2-norm error of the printer should converge because a Q is applied which makes sure there is robust convergence. The number of trails is set to 5 because it converges fast to the equilibrium point. After three iteration the controller reached its equilibrium. Furthermore, the 2-norm settles at around $12e^{-4}$ and the max error at around $6.9e^{-5}$ as can be seen in figure 4a.

g) For the next experiment L is replaced by αL. α is changing the learning speed of the ILC controller. Furthermore, α ensures a reduction in amplification trial-variant disturbances. Therefore, it should be able to reach a lower steady-state equilibrium point. The admissible range of α is computed with a perfect $L = GS^{-1}$ and $Q = 1$. When using $|Q(1 - \alpha LGS)|<1$ as condition the admissible range is $0<\alpha<2$. Otherwise the system will not converge. The smaller α is the slower the convergence is. As can be seen in figure 4b. Furthermore, the α should ensure that the amplification of the trial-variant disturbances decrease. However, this effect can not be seen in the figure. One of the problems might be that the simulation does not contain these kind of disturbances.

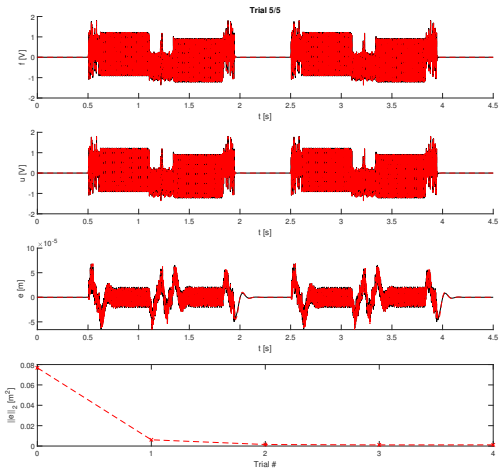

(a) Implementing ILC controller

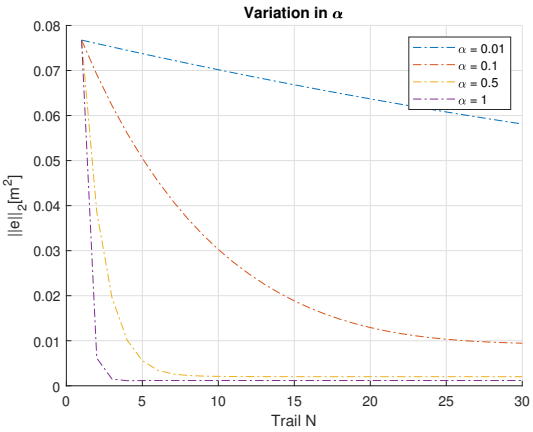

(b) Variation of α

Figure 4: Implementing ILC controller

.

Exercise 3.16 (Experiment)

a) This exercise is done with the experimental printer setup. Firstly, the mass feed forward from exercise 15.b is used to control the system with a feed forward controller. The trail is set to two again because with classical feed forward the error does not decrease after one trial. Using the same mass as exercises 15.b, $m = 0.1$ results in a small error increase. as can be seen in figure 5a. The 2-norm increases from$2.6e^{-1}$ to $2.8e^{-1}$. However, the maximum error slightly decreases from $6.8e^{-3}$ to $6.6e^{-3}$. Increasing or decreasing the mass does not have a lot of influence on the error. Furthermore, coulomb fiction is noticed in the real printer system. Therefore, this friction term is added to the feed forward. The Coulomb friction is depending on the sign of the velocity and is approximated by a linear term. Using a friction term of $K_c = 0.6$ and changing the mass to 0.7, results in the following figure 5b. As can be seen in the figure the 2-norm decreases to $3.6e^{-2}$ and the maximum value to $1.8e^{-1}$.In exercises 15.b the Coulomb friction was not needed and the mass had a different value. Therefore, the exercises had a better result.

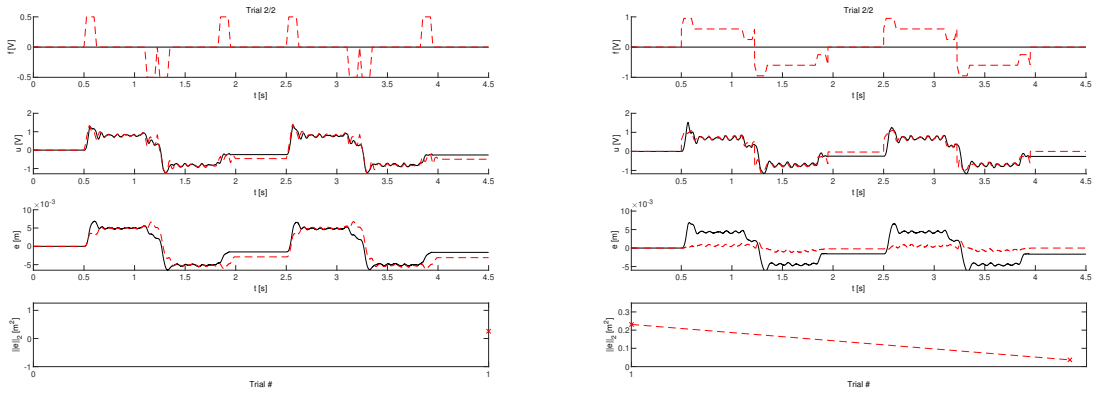

(a) Mass feed forward control

(b) Mass and Coulomb feed forward control

Figure 5: Feed forward control

b) In the second part of the experiment the previous designed controllers can be implemented on the printer. Firstly, the ILC controller is implemented with a α equal to 0.1. The max peak servo error is equal to $4.4e^{-3}$ and the 2-norm of the error is equal to $1.6e^{-1}$. There has to be a trade off between performance and robustness. This trade off can be tuned by tuning Q and α. With the setup used in this experiment the best achieved performance is with an $\alpha = 0.6$ and Q with a second order butter worth filter at 20Hz. The achieved performance can be seen in figure 6b. The corresponding errors are as follows, the peak norm error, $1.1e^{-3}$ and the 2-norm of the error, $2.1e^{-2}$.

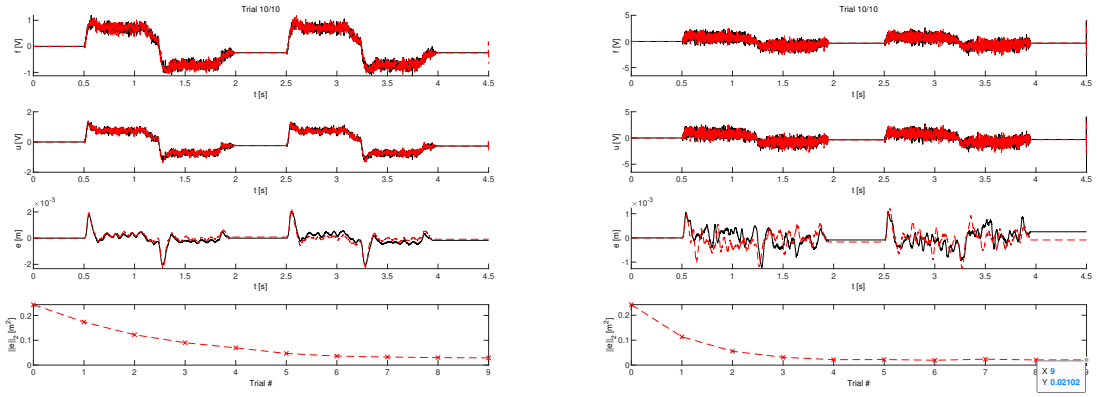

(a) ILC controller $\alpha = 0.3$

(b) ILC controller $\alpha = 0.6$

Figure 6: ILC controller tuning Q and α

Exercise 3.17

During this exercise lifted ILC is applied to the printer system.
a) The matrix J is created using the impulse response of GS and then creating a Toeplitz matrix from this impulse response. This resulted in the matrix shown in Figures 7 and 8.

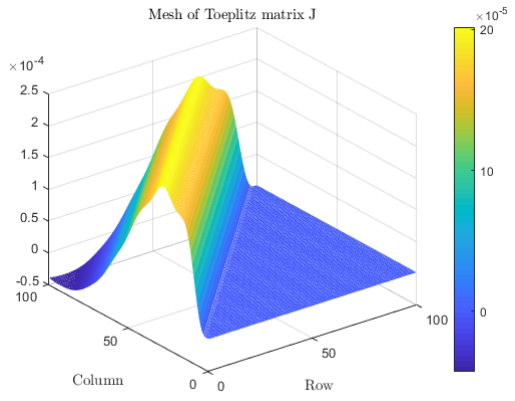

Figure 7: Mesh plot of matrix J

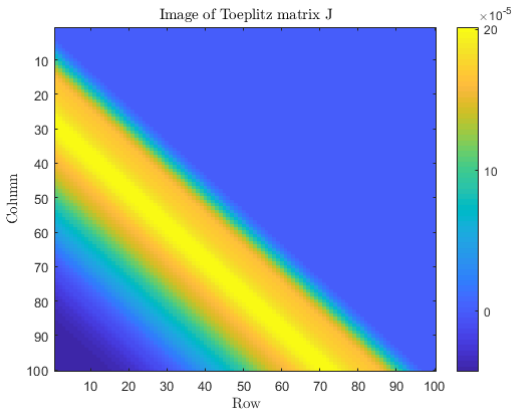

Figure 8: Image of matrix J

From these figures can be concluded that the matrix is lower triangular, Toeplitz and that the diagonal is zero. Since the impulse settles to zero, the system is stable thus proper. These properties indicate that the system is time-variant and causal.

b) Now a lifted ILC controller is designed by creating the matrices L and Q:
$X = (J^T W_e J + W_f + W_{\Delta f})^{-1}$
$Q = X(J^T W_e J + W_{\Delta f}$
$L = X(J^T W_e)$

Where:
$W_e = w_e \cdot I$, $w_e = 10^3$
$W_f = w_f \cdot I$, $w_f = 10^{-3}$
$W_{\Delta f} = w_{\Delta f} \cdot I$, $w_{\Delta f} = 10^{-1}$

This results in the matrices plotted in Figure 9 and 10.

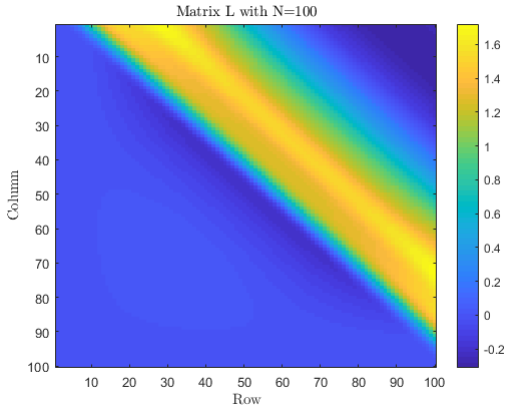

Figure 9: Matrix L

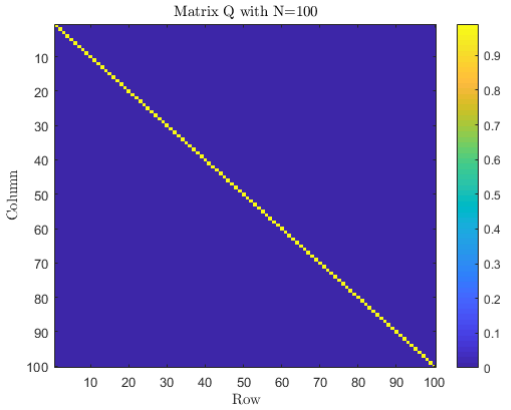

Figure 10: Matrix Q

The structure of the L matrix is upper triangular. The Q matrix is an identity matrix and both matrices have size $N = 100$. From the equation $f_{j+1} = Qf_j + Le_j$ can be concluded that Q influences the feed-forward therm f_j and Q influences the error therm e_j.

From Figure 9 can be concluded that the system is time invariant since the matrix is upper triangular, indicating that previous samples keep their value when time increases. Keeping their values also indicates causality, since the output only depends on previous inputs. Figure 10 is an identity matrix, indicating that the error values are directly fed through.

If w_f is set to zero, the future feed-forward therm f_{j+1} is not taken into the equation resulting in a slightly different L and Q matrix. Setting w_f to zero results in the adjusted L matrix shown in Figure 11 where the delta between the L matrices with $w_f = 0.001$ and 0 is plotted. The Q matrix is also adjusted as shown in Figure 12.

To guarantee that e_∞ becomes zero LJ must be non-singular: $det(LJ) \neq 0$. For the given system and weighting filters the pair LJ is singular indicating that the steady state error does not go to zero.

c) The convergence and monotonic convergence properties of the lifted ILC controller are now investigated. Convergence holds if $\max_i |\lambda_i(Q - LJ)| < 1$. Monotonic convergence holds if $\|Q - LJ\| < 1$ for any matrix norm. For example when the 2-norm is used it is determined by $\overline{\sigma}(Q - LJ) < 1$.

For the designed lifted ILC controller (with w_f) both the convergence and monotonic convergence properties hold. When w_f is set to zero, both the convergence and monotonic convergence do not hold anymore. The equations to determine convergence and monotonic convergence both become 1, where they where below 1 first with $w_f > 0$.

d) Now the lifted ILC controller is implemented in the printer setup simulation. For this N is set to 4501, the sample length of the servo task. During this experiment the influence of w_e, w_f and $w_{\Delta f}$ on

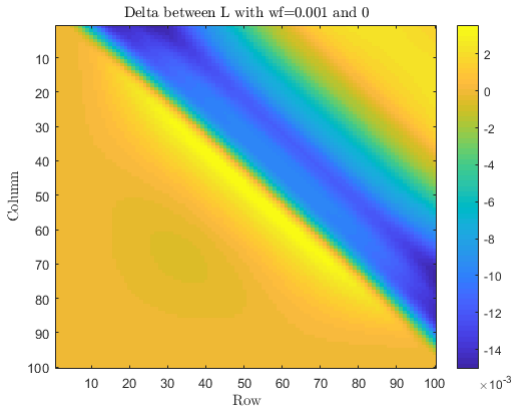

Figure 11: Matrix L delta

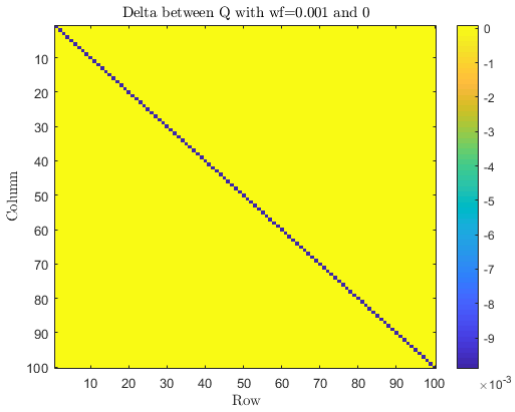

Figure 12: Matrix Q delta

convergence speed and ILC performance is investigated.

To determine the influence of each parameter, they are individually adjusted and the error norm is examined. Initially, the same filter coefficients as used during exercise 17b are used while one of the three parameters is adjusted. This resulted in the convergences shown in Figure 13.

Increasing W_e resulted in a faster convergence and also a lower error norm. Decreasing W_f also resulted in faster convergence, however the difference between 10^{-5} and 10^{-3} is small compared to the difference in convergence between 10^{-3} and 10^{-1}. Decreasing $W_{\Delta f}$ also resulted in faster convergence and a lower error norm.

e) Now the lifted ILC controller is compared to the frequency domain ILC controller. To design the lifted ILC controller for zero converged error, the weighting filter W_e must have the highest possible gain and $W_f, W_{\Delta f}$ must have the lowest possible gains while the system is still converging. To attenuate trial varying disturbances, weight $W_{\Delta f}$ must be decreased because this weight is multiplied with the difference in current and next feed-forward therm. Addressing model errors is done by increasing W_f, setting W_f to zero is done when there are no modelling errors. For the frequency domain ILC controller: obtaining zero converged error is possible if $Q = 1$, however this is a trade-off between robustness because $|Q(1 - GSL)| < 1$ must hold.
For the frequency domain ILC, the response of the system must be simulated for each iteration based on the model of the system. This does not use as many computational resources as multiplying the matrices L and Q for the lifted ILC case. For frequency domain ILC controller is causal, however it is made noncausal since the samples are shifted in matrix L. In the lifted ILC case, the delay of the system can also be found in matrix J and thus in matrix L.

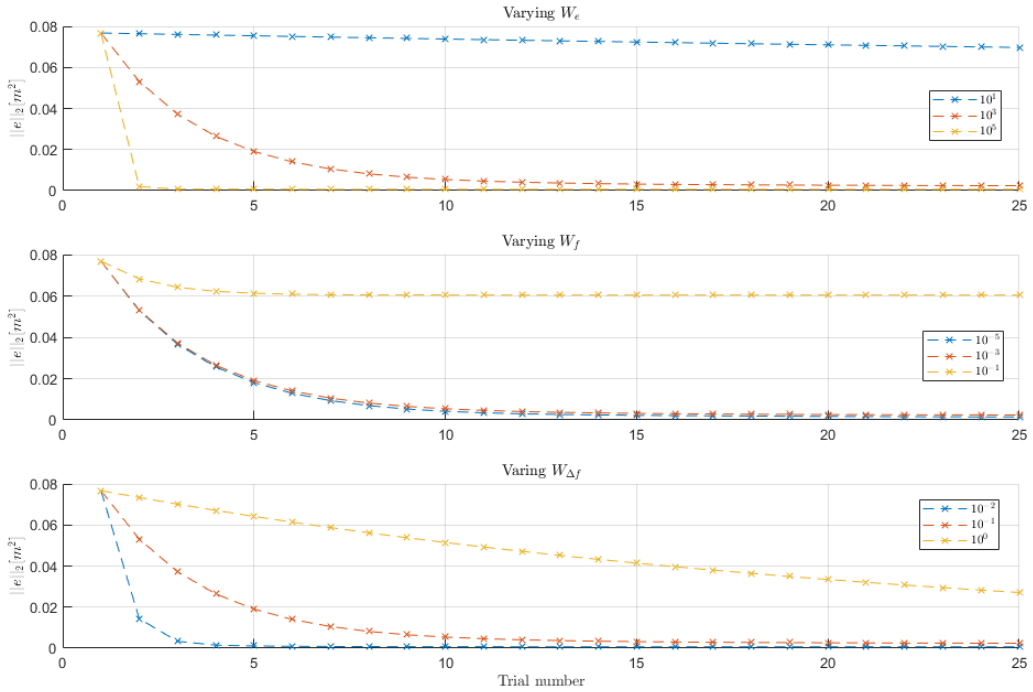

Figure 13: Influence of weighting filter parameters on convergence

.

Exercise 3.18

In this exercise the ILC controller $f_{j+1} = Qf_j + Le_j$ is examined with $J = 1$, $Q = -0.8$, $L = -0.4$, trial length $N = 1$ and reference $r = 1$. The convergence and monotonic convergence of this controller are investigated during 20 iterations while plotting e_k and f_k.

Convergence is determined by $\max_i |\lambda_i(Q - LJ)| < 1$, resulting in 0.4 indicating that convergence holds. The monotonic convergence is determined by $\overline{\sigma}(-0.4) < 1$, which results in 0.16. However, the system does not convert monotonically and the error e_j also increases as shown in Figure 14.

This behavior results from the steady state error: $e_\infty = \left(I_{NI} - J\left(I_{NI} - Q + LJ\right)^{-1} L\right) r$, resulting in $e_\infty = 1.286$ using the given ILC controller. The combination of negative Q and L matrices result in this steady state error that the systems error converges towards as shown in Figure 15.

In conclusion it is needed to also compute the steady state error e_∞ to conclude monotonic convergence.

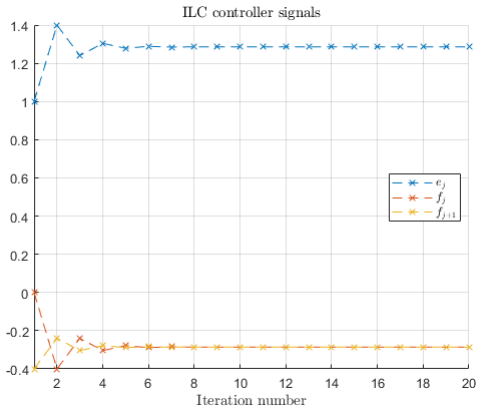

Figure 14: Response of system

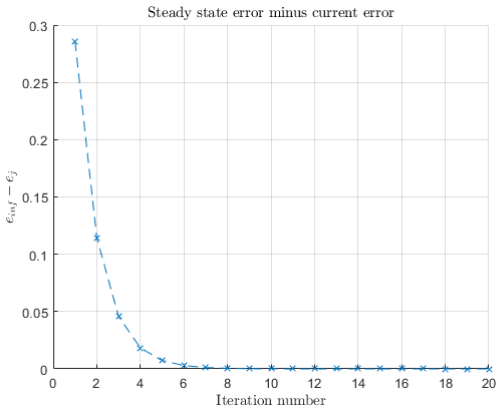

Figure 15: Convergence of error towards steady state error

Exercise 3.19

For lifted ILC monotonic convergence is often with respect to the vector 2-norm of the error. In this exercise there is investigated if monotonic convergence in a vector norm implies monotonic convergence in another norms. Monotonic convergence of the error is achieved if the condition $\|e_\infty - e_{j+1}\| \leq k \|e_\infty - e_j\|$ holds for $0 \leq k<1$ in equation 6 is not exceeded.

$$J = \begin{bmatrix} -1 & 0 \\ 0 & -1 \end{bmatrix} \quad Q = \begin{bmatrix} 1 & 0 \\ 0 & 1 \end{bmatrix} \quad L = \begin{bmatrix} -\frac{1}{4} & \frac{1}{2} \\ 0 & -\frac{3}{4} \end{bmatrix} \tag{4}$$

$$J = \begin{bmatrix} -1 & 0 \\ 0 & -1 \end{bmatrix} \quad Q = \begin{bmatrix} 1 & 0 \\ 0 & 1 \end{bmatrix} \quad L = \begin{bmatrix} -\frac{1}{4} & 0 \\ \frac{1}{2} & -\frac{3}{4} \end{bmatrix} \tag{5}$$

$$||Q - LJ|| < 1 \tag{6}$$

For system two, 5. The matrix 1-norm does not conform to the condition from 6, $||Q - LJ||_{i1} = 1.25$. Therefore, the 1-norm of the error is not monotonic convergent. Furthermore, the 2-norm and ∞-norm do conform to the condition. For system one (4) $||Q - LJ||_{i\infty} = 1.25$, which ensures the ∞-norm does not monotonically converges. The other norms do hold to the condition and are therefore, monotonically converging. In the figure 16 the exceeding of the 1-norm for system 2 and the ∞-norm for system 1 can be seen.

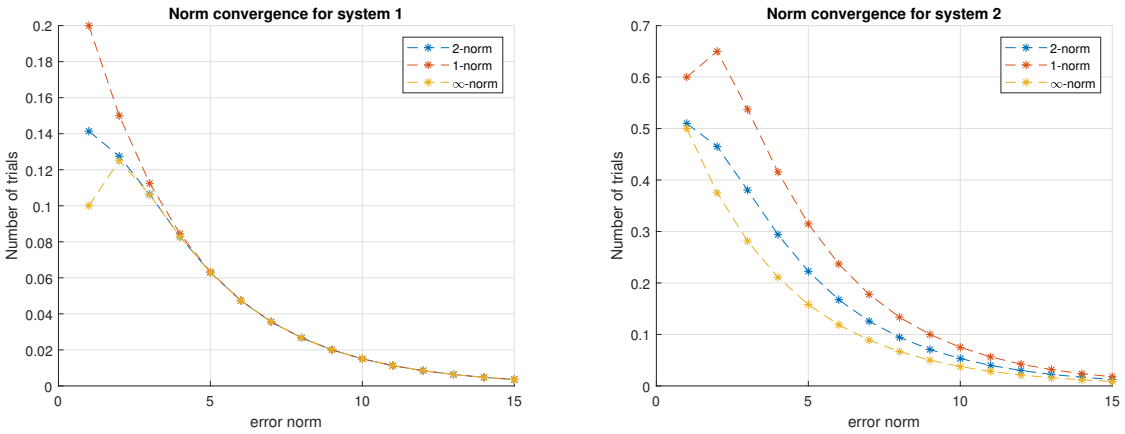

(a) Convergence of norms system 1

(b) Convergence of norms system 2

Figure 16: Norm convergence

Exercise 3.20

In this exercise the following system is considered:

$$J(z) = \left[\begin{array}{c|c} A & B \\ \hline C & D \end{array}\right] = \left[\begin{array}{c|c} 0.5 & 1 \\ \hline 1 & 1 \end{array}\right]$$

and it is controlled by the ILC controller $f_{j+1} = Qf_j + Le_j$ where $Q = 1$ and $L = \alpha$.

1) The system is convergent for α values of $0 < \alpha < 2$ because of the convergence ($\max_i |\lambda_i(Q - LJ)| < 1$) and monotonic convergence properties ($\overline{\sigma}(Q - LJ) < 1$).
2) Now the ILC controller is implemented in finite time with $N = 2$. This results in the admissible range of α for convergence of $0 < \alpha < 2$ because in this range the equation $\max_i |\lambda_i(Q - LJ)| < 1$ holds. The admissible range of α for monotonic convergence is $0 < \alpha < 1$ because then $\overline{\sigma}(Q - LJ) < 1$ holds. **3)** The admissible range of α to guarantee convergence on a finite time interval N is still $0 < \alpha < 1$ since for convergence only the maximum eigenvalue counts, which is always 0.5. However, the admissible range of α to guarantee monotonic convergence on a finite time interval N is now $0 < \alpha < \frac{2}{3}$, since the 2-norm of the matrix $Q - LJ$ is now increased by all the extra entries. This maximum value is computed using the $\|H\|_\infty$ norm of the system, which is 3. This results in a maximum α of $\frac{2}{3}$.

4) Now a lifted ILC with $\alpha = 0.75$ and $N = 2$ is used, however the states of $J(z)$ are not reset after every trial and the system is excited by a periodic signal $r(k)$, where $r(k + N) = r(k)$. The Nyquist stability theorem for RC can be used to conclude on stability of this system. S_r as in equation 7 is considered to be stable if the Nyquist plot of $-z^{-N}Q(z)(1-T(z)L(z))$ makes no encirclement's of the point -1 and does not pass through the -1 point.

$$S_R = \frac{1 - z^{-N}Q(z)}{1 - z^{-N}Q(z)(1 - T(z)L(z))} \tag{7}$$

5) The same question as **4**, however now $N = 3$. This is not tested anymore.